© 2014. Published by The Company of Biologists Ltd | Journal of Cell Science (2014) 127, 3983–3997 doi:10.1242/jcs.149336

RESEARCH ARTICLE

Sortilin mediates the release and transfer of exosomes in concert with two tyrosine kinase receptors

Cornelia M. Wilson[1,*,‡], Thomas Naves[1,*], François Vincent[1,2], Boris Melloni[2], François Bonnaud[2], Fabrice Lalloué[1] and Marie-Odile Jauberteau[1]

ABSTRACT

The transfer of exosomes containing both genetic and protein materials is necessary for the control of the cancer cell microenvironment to promote tumor angiogenesis. The nature and function of proteins found in the exosomal cargo, and the mechanism of their action in membrane transport and related signaling events are not clearly understood. In this study, we demonstrate, in human lung cancer A549 cells, that the exosome release mechanism is closely linked to the multifaceted receptor sortilin (also called neurotensin receptor 3). Sortilin is already known to be important for cancer cell function. Here, we report for the first time its role in the assembly of a tyrosine kinase complex and subsequent exosome release. This new complex (termed the TES complex) is found in exosomes and results in the linkage of the two tyrosine kinase receptors TrkB (also known as NTRK2) and EGFR with sortilin. Using *in vitro* models, we demonstrate that this sortilin-containing complex exhibits a control on endothelial cells and angiogenesis activation through exosome transfer.

KEY WORDS: Sortilin, Exosome, Cancer, EGFR, TrkB, NTRK2, Angiogenesis

INTRODUCTION

Cancer cells influence their cellular microenvironment through intercellular communication. Growing evidence indicates that microenvironment control is supported by the release of extracellular microvesicles called exosomes. Exosomes are small membrane-bound vesicles, ranging in size from 40 to 100 nm that are derived from endosomes (Pan et al., 1985). They have the ability to transfer their cellular content to neighboring cells and to modify the microenvironment to promote tumor-induced immune suppression, angiogenesis and pre-metastatic niche formation (Simons and Raposo, 2009; Théry et al., 2009). The role of exosomes is likely to be dictated by their contents, which are composed of microRNAs (miRNAs), RNAs, lipids and more than 400 proteins. However, the function of some of these exosomal proteins is as yet unknown.

The multifaceted receptor sortilin (also known as neurotensin receptor 3) plays a multitude of roles in the cell, as a receptor or co-receptor, in the transport of proteins such as neurotensin and neurotrophins to the plasma membrane and to lysosomes, and in regulated secretion (Nykjaer and Willnow, 2012). A number of reports have shown that sortilin expression is elevated in several human cell lines (Dal Farra et al., 2001; Giorgi et al., 2008; Truzzi et al., 2008). Some of these reports have suggested that sortilin can play a dual role through its direct interaction with neurotensin or with mature neurotrophin receptors in cells that stimulates an autocrine and/or paracrine function, which could be a mechanism associated with cell survival and tumorigenesis (Dal Farra et al., 2001; Truzzi et al., 2008). A growing number of reports have highlighted that there can be metalloproteinase-mediated shedding of the extracellular domain of sortilin into the culture medium in several cell types (Hermey et al., 2006; Massa et al., 2013; Navarro et al., 2002). However, the mechanism of sortilin release from these cells and the consequence for the microenvironment is uncertain. In this study, we examined closely the secretion mechanism involved in the release of the extracellular domain of sortilin from human lung cancer cells (A549), together with the effect on endothelial cells. We show for the first time that sortilin is a key component of exosome-mediated communication between A549 and endothelial cells. Using *in vitro* models, we demonstrate that sortilin is essential for exosome release and is involved in the assembly of a new complex containing two tyrosine kinase receptors, which is increased in non-small cell lung cancer. This complex comprises tropomyosin-related kinase B (TrkB, also known as NTRK2), which is implicated in the activation and invasion of A549 lung cancer cells through the binding of the brain-derived neurotrophin factor (BDNF) (Zhang et al., 2010), and epidermal growth factor receptor (EGFR) (Mendelsohn and Baselga, 2003), both associated with sortilin. This newly reported TrkB–EGFR–sortilin (TES) complex in exosomes has a function in the activation and migration of endothelial cells and could play a role in lung cancer angiogenesis.

RESULTS

Sortilin is processed and released from HEK293 and A549 cells

Sortilin, a member of the Vps10p domain family of receptors, is a type 1 membrane protein receptor (Fig. 1A). It is expressed in most tissues, notably the brain, central nervous system, muscle and other peripheral cell types. The expression of sortilin is upregulated in a number of cancers including breast, colon and prostate cancer. Sortilin exists in two forms, a full-length form (110 kDa) and a truncated form (95 kDa), corresponding to its large luminal domain (or ectodomain), which has been previously detected in the supernatant medium from sortilin-overexpressing cells (Navarro et al., 2002). To determine whether shedding of the ectodomain of sortilin occurs, we evaluated the expression of

[1]EA3842 Homéostasie Cellulaire et Pathologies and Chaire de Pneumologie Expérimentale, Université de Limoges, Faculté de Médecine, 2 Rue du Dr Raymond Marcland, 87025 Limoges CEDEX–France. [2]Service de Pathologie Respiratoire, Centre Hospitalier et Universitaire de Limoges, 87000 Limoges CEDEX-France.
*These authors contributed equally to this work

‡Author for correspondence (cornelia.wilson@unilim.fr)

Received 13 January 2014; Accepted 7 July 2014

Journal of Cell Science

Journal of Cell Science (2014) 127, 3983–3997 doi:10.1242/jcs.149336

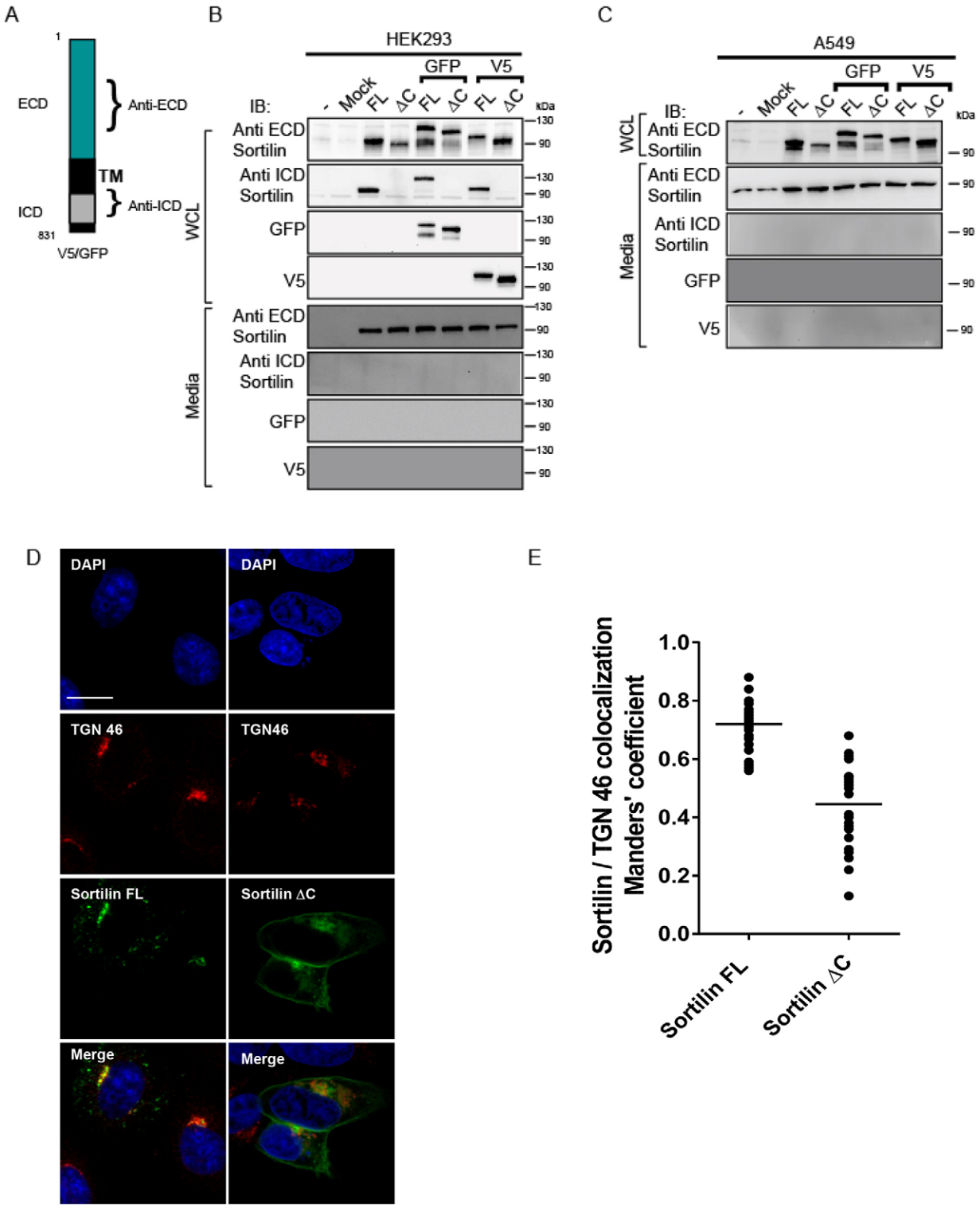

Fig. 1. Sortilin is released from HEK293 and A549 cells. (A) Schematic representation of sortilin topology showing the sites of antibody epitope binding. ECD, ectodomain; ICD, intracellular domain. (B,C) HEK293 cells (B) or A549 cells (C) were transfected with full-length (FL) or truncated (ΔC) sortilin with or without GFP or V5 epitope tags. The whole-cell lysate (WCL) and medium samples were collected at 24 h post-transfection. Medium samples were precipitated with trichloroacetic acid (TCA) and all samples were analyzed by western blotting using antibodies specific to either the ectodomain (anti-ECD) or intracellular domain (anti-ICD) of sortilin, or the GFP or V5 epitope tags. (D) A549 cells were transfected with full-length or truncated GFP-tagged sortilin and stained for the indicated proteins and with DAPI. Scale bar: 10 μm. (E) Manders' coefficient indicating a colocalization between sortilin and TGN46. Data represent the range of values obtained from two independent experiments with at least 15–30 cells.

Journal of Cell Science (2014) 127, 3983–3997 doi:10.1242/jcs.149336

different sortilin constructs in two cell lines, human embryonic kidney cells (HEK293), to validate the constructs used in previous studies (Finan et al., 2011; Nielsen et al., 2001), and the cell line of interest, lung adenocarcinoma epithelial cells (A549). We observed that human kidney cells expressed a low endogenous level of full-length sortilin (110 kDa) (Fig. 1B), detected using an ectodomain-specific antibody against sortilin. In order to observe sortilin expression, we expressed various tagged and untagged versions of full-length and C-terminally truncated constructs of sortilin in HEK293 cells. It is interesting to note that the cytoplasmic tail of sortilin encodes two sorting motifs, a tyrosine-based YSVL motif and an acidic dileucine cluster motif, which facilitate both endocytosis and intracellular trafficking of sortilin (Nielsen et al., 2001). Full-length sortilin (110 kDa), when overexpressed and tagged either with GFP (130 kDa) or V5 (115 kDa), was detected in HEK293 cells (Fig. 1B), whereas immunopositive 95-kDa sortilin products were only detected in the medium (using the ectodomain-specific antibody) (Fig. 1B). Truncation of the C-terminus of sortilin results in the generation of smaller products at ~95 kDa. We verified that these products still contained their appropriate tags using antibodies against GFP and V5 (Fig. 1B). We found truncated sortilin in the medium only with the ectodomain-specific antibody, with the loss of GFP- and V5-tagged proteins further indicating shedding of the C-terminus (Fig. 1B). Likewise, when we performed the same analysis in lung cancer cells (A549), we obtained similar results regarding the loss of tagged sortilin and the shedding of sortilin into the medium (Fig. 1C). To determine the subcellular localization of sortilin, we performed an immunocytochemistry analysis of both full-length and cytoplasmic-truncated sortilin in A549 cells. At 18 h post-transfection of GFP-tagged full-length and truncated sortilin, we found that full-length sortilin localized to the perinuclear region, such as in the trans-Golgi network (TGN), as confirmed by analysis of the colocalization with a TGN marker TGN46, which gave a high Manders' coefficient (Fig. 1D,E). Truncated sortilin distribution was more widespread, with notable peripheral and cell surface localization, and the analysis of its colocalization with TGN46 gave a lower Manders' coefficient (Fig. 1D,E). Hence, the shedding of sortilin and its subcellular localization in A549 cells (Fig. 1C,D) is in accordance with previous reports (Finan et al., 2011; Nielsen et al., 2001).

Sortilin is secreted in exosomes

To gain further insight into the mechanism used for sortilin release into the medium, we first analyzed the transport routes that sortilin could use for secretion from the cell. One such possible route that sortilin could use is through exosomes, which are actively secreted through an exocytosis pathway normally used for receptor discharge and intercellular cross-talk (Raposo and Stoorvogel, 2013; Record et al., 2014). In order to confirm that A549 cells secrete exosomes into the culture medium, we first checked for the cell expression of the tetraspanin proteins CD63 and CD81, which are enriched in late endosomes and abundant in exosomes (Escola et al., 1998; Raposo et al., 1996). These were detected by fluorescence-activated cell sorting (FACS) after staining for CD63 and CD81 with fluorescent antibodies, or for EGFR, an exosome marker (supplementary material Fig. S1). To screen for exosomes secreted from A549 cells, we used two procedures. The first was the previously developed FACS-based assay (Ostrowski et al., 2010). In brief, exosomes present in the culture medium were captured onto beads coated with an antibody to the exosome marker CD63, and were detected by FACS after staining with for CD81 with fluorescent antibodies. Thus, we showed that A549 cells secrete exosomes into the culture medium (Fig. 2A). We used a number of compounds that are known to affect protein transport and stimulate secretion at different stages. Brefeldin A (BFA) is known to affect the classical protein transport pathway, preventing anterograde traffic from the endoplasmic reticulum (ER) to the Golgi and resulting in retrograde transport of proteins from the Golgi to the ER (Lippincott-Schwartz et al., 1989; Wilson et al., 2011). As shown in Fig. 2B, treatment with 1 µg/ml BFA had a major effect on sortilin release in exosomes into the medium under basal conditions. Likewise, treatment with the antibiotic tunicamycin, which inhibits synthesis of the lipid-linked oligosaccharide precursor important for glycoprotein traffic from the ER and Golgi compartments, prevented the release of sortilin into the medium (Fig. 2B). When cells were treated with dimethyl amiloride (DMA), which is known to perturb secretion (Savina et al., 2003), exosomes isolated from A549 cells showed a marked reduction in sortilin (Fig. 2B). We next tested the effect of a reagent called Monensin (Mon), previously shown to affect exosome secretion (Savina et al., 2003). We observed that Mon treatment significantly reduced intracellular levels of sortilin and potentiated the secretion of sortilin into the medium (Fig. 2B). We obtained similar results to those observed with sortilin for EGFR in whole-cell lysates and exosomes under the different treatments (Fig. 2B). The second procedure is a quantitative CD63 and CD81 enzyme-linked immunosorbent assay (ELISA)-based analysis, which involves an ultracentrifugation step to harvest exosomes from culture medium. As shown in Fig. 2C, the average number of exosome particles in control conditions for CD63 and CD81 that were obtained per ml of A549 culture medium was $\sim 4\times10^9$. We observed a significant reduction in the exosome population for both CD63 and CD81 secreted from A549 cells when using the chemical inhibitors BFA (CD63, $P=0.001$; CD81, $P=0.0009$), tunicamycin (CD63, $P=0.0006$; CD81, $P=0.0009$) and DMA (CD63, $P=0.0057$; CD81, $P=0.0084$) (Fig. 2C). In contrast, Mon treatment resulted in a significant elevation of secreted exosomes (CD63, $P=0.005$; CD81, $P=0.006$) (Fig. 2C). To establish that sortilin is secreted through endocytic exosomes, we purified the exosome population secreted by A549 cells. Western blotting carried out on the exosomal extracts confirmed the presence of exosomal proteins known to be enriched in A549 exosomes, such as the multivesicular body (MVB) marker Tsg101, which is important for membrane protein transport (Babst et al., 2000) and indicates an endosomal origin of the vesicles, the molecular chaperone heat shock protein 90 (Hsp90) and the exosomal protein flotillin (Fig. 2D). We confirmed that sortilin, in particular its extracellular domain, is enriched in A549 exosomes (Fig. 2D). Next, we immunocaptured purified exosomes with anti-CD63 or non-related-serum-coated beads followed by western blotting with for the ectodomain of sortilin (Fig. 2E). The results further confirmed that sortilin is secreted through endocytic exosomes. To prove that intracellular sortilin localizes to late endosomal membranes, we performed electron microscopy analysis using immunogold labeling against the sortilin protein on ultrathin cryosections of A549 cells. Fig. 2F shows unlabeled images obtained from A549 cells, including whole cells and MVBs, facilitating identification of organelle structures. Fig. 2G also shows localization of sortilin (5-nm gold particles) to intraluminal vesicles (ILVs), with the average ILV size of 48 nm within MVBs. Higher magnification showed that sortilin protein was localized to ILVs and to the outer membrane of MVBs (Fig. 2G). When we performed similar EM immunogold

Journal of Cell Science (2014) 127, 3983–3997 doi:10.1242/jcs.149336

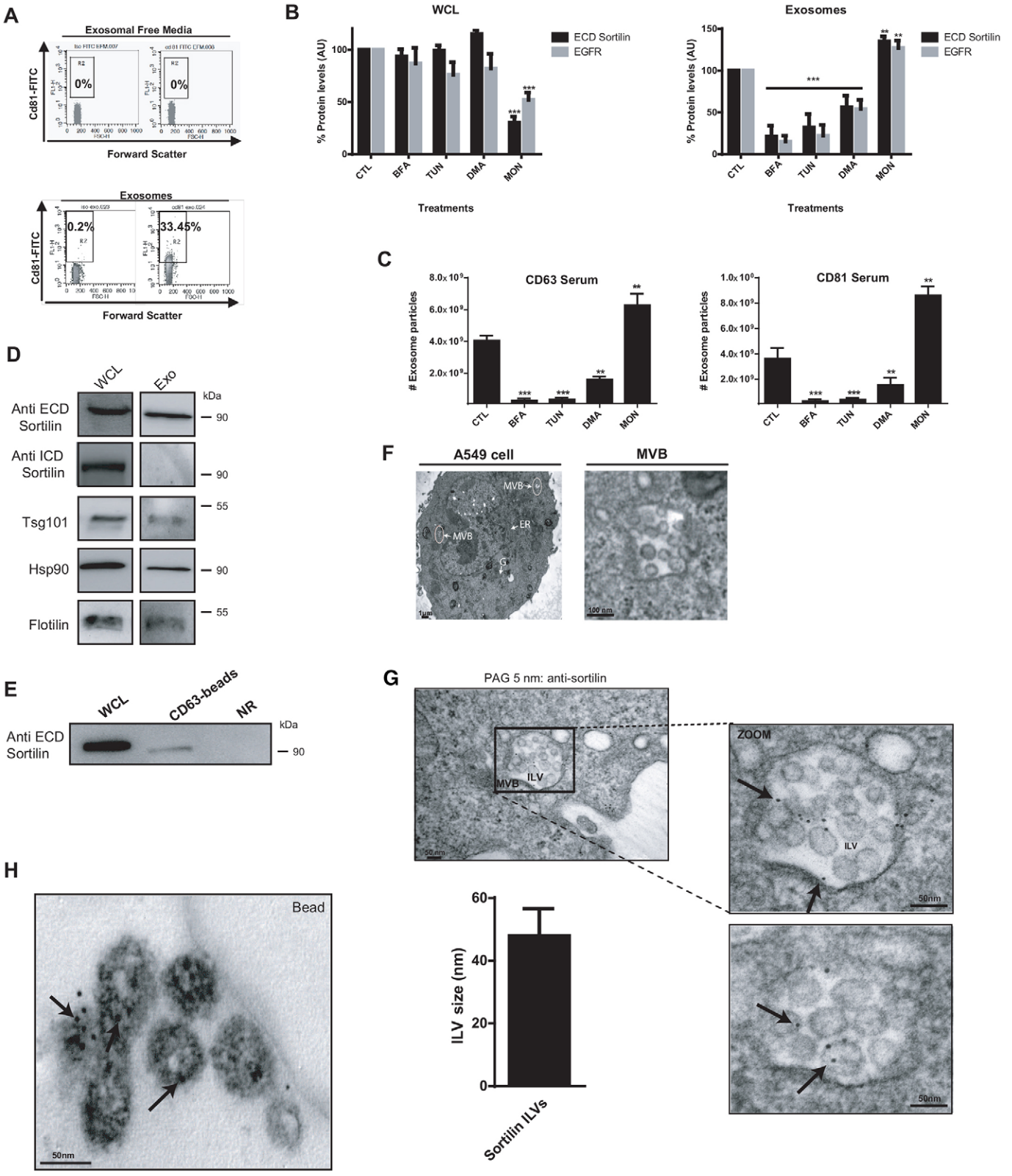

Fig. 2. See next page for legend.

labeling of CD63-purified exosomes, we found that sortilin was localized to CD63-positive exosomes (Fig. 2H). Taken together, our results confirm that sortilin is found in MVBs and is secreted from the cell in exosomes.

Sortilin is a key component for the release of A549 exosomes

To investigate whether sortilin plays a role in A549 exosomes, we generated stable knockdowns of sortilin and Rab27a, a small Rab GTPase involved in MVB docking at the plasma membrane, as a

Journal of Cell Science

Journal of Cell Science (2014) 127, 3983–3997 doi:10.1242/jcs.149336

Fig. 2. Sortilin is found in exosomes. (A) Flow cytometry dot-plots showing isotypic and CD81 (left), and CD63 and CD81 (right) staining of exosomes captured by beads incubated with supernatants from exosome-free medium (top) and A549 exosomes (bottom). (B) Quantification of the ectodomain (ECD) of sortilin and EGFR protein levels in whole-cell lysate (WCL) and exosomes from A549 cells (2.5×10^5) after treatment as indicated for 24 h, analyzed for statistical significance with a Student's *t*-test. $^{**}P<0.01$; $^{***}P<0.001$. TUN, tunicamycin; MON, Monensin. (C) A549 cells (2.5×10^5) were treated as detailed above. Exosome quantification was performed using an ELISA-based assay of CD63 (left) or CD81 (right) and analyzed for statistical significance with a Student's *t*-test. $^{**}P<0.01$; $^{***}P<0.001$. (D) A549 cells and medium were harvested at 24 h post-transfection with full-length sortilin. Whole-cell lysate was prepared from A549 cells and exosomes (Exo) were purified by ultracentrifugation from the medium, followed by western blot analysis for the sortilin ECD, the sortilin ICD, Tsg101, Hsp90 and flotillin. (E) Exosomes were purified and then immunocaptured with CD63-coated beads or non-related serum (NR) followed by western blotting with anti-ECD sortilin antibody. (F,G) Electron microscopy analysis of A549 cells and ultrathin sections stained with sortilin antibody using protein-A gold (PAG) particles with the size of 5 nm. (F) Left, electron microscopy image of an A549 cell with multiple late endosomes (MVBs). Golgi (G), ER and ILVs are shown. Right, magnification showing an MVB containing ILVs. (G) Top panel and zoom images (right) show sortilin (5-nm gold particles) localized to ILVs and to the outer membrane of MVBs (indicated by the black arrows). Bottom left, quantification of average sortilin-containing ILV size. (H) Electron microscopy analysis of exosomes present on the surface of anti-CD63-coated beads followed by immunogold labeling with sortilin. Arrows show sortilin localized to the surface of exosomes.

control for blocking the exosome release, using short hairpin RNA (shRNA) (Peinado et al., 2012). We confirmed the efficiency of sortilin and Rab27a knockdown compared to pLKO control by measuring both mRNA and protein levels (Fig. 3A,B). Exosomes were purified by differential ultracentrifugation and quantified by CD63 and CD81 ELISA from the culture medium of cells stably expressing one of two shRNAs against sortilin or an shRNA against Rab27a. We observed a significant decrease in the exosome population for both CD63 and CD81 secreted from A549 cells stably expressing shRNA for both sortilin and Rab27a (Fig. 3C).

We analyzed the subcellular distribution of CD63 by immunofluorescence in A549 cells (supplementary material Fig. S2A). In a comparison of the control and Rab27a-knockdown cells, CD63, a marker of MVBs, appeared to be homogenously distributed throughout the cell, but the intensity and clustering was more noticeable with Rab27a silencing (supplementary material Fig. S2A). Likewise, sortilin-knockdown cells showed a similar staining pattern to Rab27a, where the intensity of CD63 staining was different from control. In contrast, the knockdown of the Golgi-localized protein γ-adaptin ear-containing, ARF-binding 1 (GGA1) caused perinuclear CD63 staining with some clustering, compared to the control (supplementary material Fig. S2A). Furthermore, quantitative analysis of CD63–FITC fluorescence revealed that both sortilin- and Rab27a-knockdown cells had significantly higher CD63 staining compared to the pLKO control (supplementary material Fig. S2B). Pulse-chase analysis of CD63 over a 24-h period demonstrated that sortilin knockdown impaired exosome secretion from A549 cells, as observed by CD63 accumulation in the cells and a reduction in the amount of CD63-enriched exosomes released into the culture medium (Fig. 3D,E). Surprisingly, electron microscopy analysis revealed that the number of ILVs found in MVBs was significantly increased in sortilin-knockdown cells compared to those observed from pLKO control cells (Fig. 3F). In addition, the sortilin phenotype resulted in larger ILVs than those observed in pLKO control cells (Fig. 3F). Likewise, we observed an increased population of ILVs in MVBs after Rab27a knockdown (Fig. 3F). In contrast, analysis of ILVs in Rab27a-knockdown cells revealed no change in the surface area of the ILVs compared to pKLO control, whereas the surface area was significantly smaller than that observed after sortilin knockdown (Fig. 3F). Both the pulse-chase and immunofluorescence analysis indicate that CD63 secretion is perturbed in sortilin-depleted cells. To examine the CD63 exosome population more closely, we performed a sucrose density gradient analysis (supplementary material Fig. S2C). After exosome purification, the 100,000 ***g*** exosome pellet was fractionated through an overlaid sucrose gradient where CD63-positive exosomes have been shown to sediment at ~1.10–1.19 g/ml (Bobrie et al., 2012). Similarly, we observed that CD63-positive exosomes fractionated at between 1.10 and 1.19 g/ml, with a peak in the 1.13 g/ml fraction, along with EGFR and flotillin (supplementary material Fig. S2C). In contrast, both sortilin and Rab27a shRNA impaired the secretion of CD63-positive exosomes compared to the pLKO control (supplementary material Fig. S2C). However, in the case of sortilin shRNA, we observed that a population of exosomes remained, as judged by the presence of flotillin within the exosome fractions (supplementary material Fig. S2C). These results show that the number of ILVs observed per MVB was significantly increased after both sortilin and Rab27a knockdown. In contrast, the size of ILVs in the MVBs was much larger with sortilin shRNA than those observed with Rab27a shRNA, highlighting the different role(s) played by sortilin and Rab27a in MVB maturation and exosome secretion. These results are the first documented evidence of the importance of sortilin in controlling exosome secretion from A549 cells.

Analysis of exosome transfer and a new sortilin complex found in exosomes

To investigate the capacity of cells to take up exosomes, we utilized human umbilical vein endothelial cells (HUVECs) as target cells. First, we assessed whether exosomes could be incorporated into the target cell. We collected A549 conditioned cell culture medium after 48 h and purified the exosome fraction. The exosomes were then labeled with a low-density-lipoprotein dye (DiI), and HUVECs that had been transfected with turbo-green were incubated with the labeled exosomes for 24 h. We performed a *z*-stack analysis and found that exosomes were incorporated into HUVECs (supplementary material Fig. S3A). In a more detailed study, we examined the fate of exosomes. Purified exosomes were labeled with the dye PKH67 and added to HUVECs. After incubating HUVECs with exosomes prepared from the pLKO control for 3 h at 37℃, cells were fixed and analyzed by confocal microscopy. We observed efficient internalization of pLKO exosomes by HUVECs (Fig. 4A,B), which could be blocked by pre-treating HUVECs with the dynamin inhibitor dynasore or by keeping the cells at 4℃ during the incubation (Fig. 4A,B). When HUVECs were incubated with exosomes derived from sortilin-knockdown cells, the level of exosome uptake was significantly reduced. Likewise, Rab27a knockdown affected exosome uptake into HUVECs (Fig. 4A,B). We next analyzed whether we could observe the transfer of sortilin-containing exosomes to HUVECs. To facilitate this analysis and to improve the sensitivity of the assay, we chose to perform a 2-day pulse-chase experiment (Fig. 4C). In brief, sortilin was overexpressed in A549 cells by transient transfection and, at 18 h post-transfection, a pulse-labeling was performed for 5 h followed by a 24-h chase. After the

Journal of Cell Science (2014) 127, 3983–3997 doi:10.1242/jcs.149336

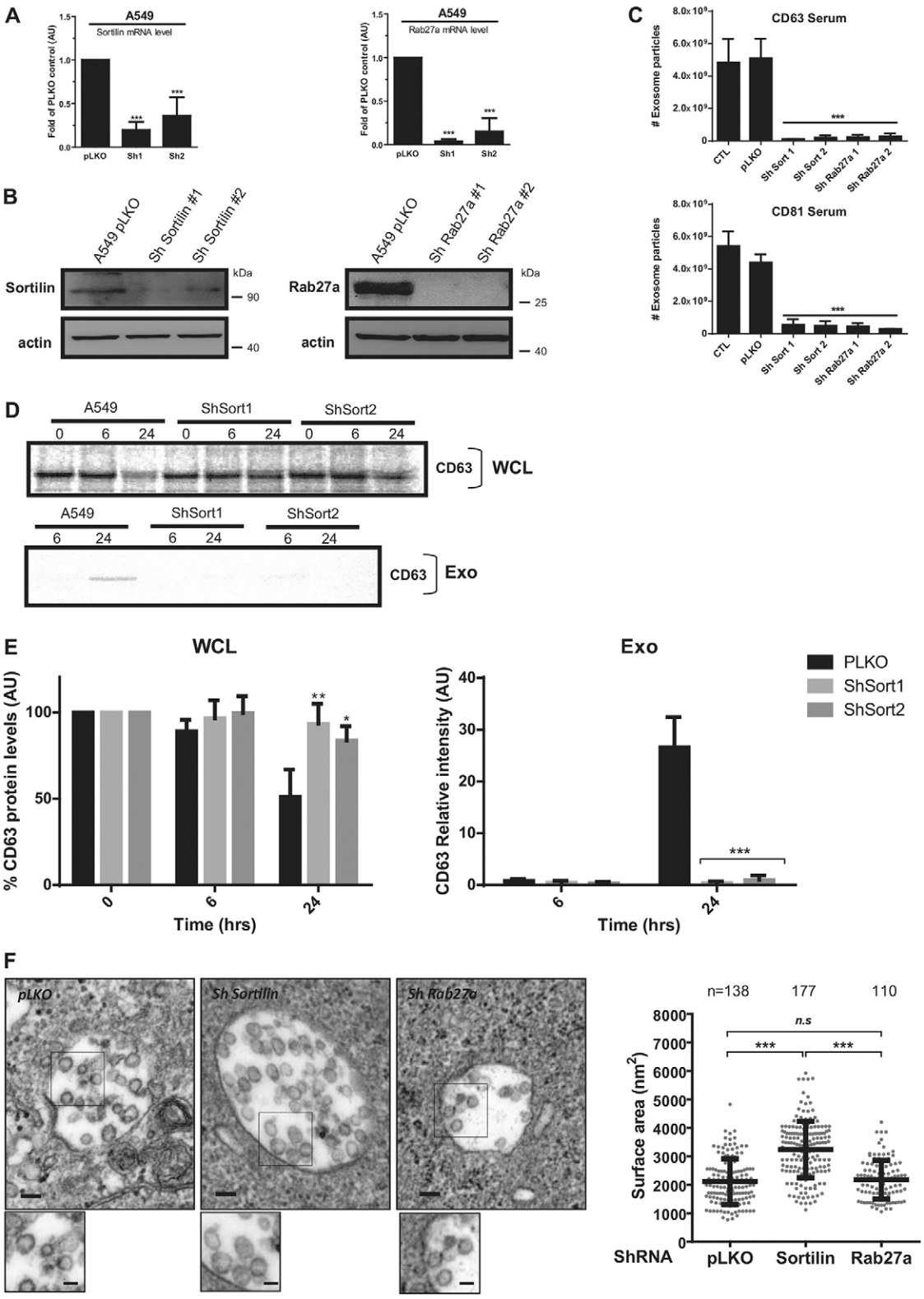

Fig. 3. See next page for legend.

24-h chase, we harvested the labeled A549 exosomes from the culture medium by differential centrifugation and incubated HUVECs with the labeled exosomes for 24 h. Remarkably, after immunoprecipitation with the ectodomain-specific sortilin antibody, we pulled-down two labeled SDS-resistant products in A549 cells expressing sortilin, which migrated at between ~350–400 kDa (Fig. 4D, A549 WCL lane). Interestingly, the higher product (~400 kDa) was secreted from A549 in exosomes

Journal of Cell Science (2014) 127, 3983–3997 doi:10.1242/jcs.149336

Fig. 3. Sortilin is essential for exosomal release. (A) Levels of mRNA encoding for sortilin and Rab27a as determined by quantitative RT-PCR in human A549 cells after expression of shRNAs for pLKO (control), shRNA no. 1 and no. 2 (Sh1, Sh2) for sortilin and Rab27a. The mRNA level of sortilin (left) or Rab27a (right) is expressed in arbitrary units (AU) as compared with pLKO control, and was analyzed for statistical significance with a Student's *t*-test. ***$P<0.001$. (B) Expression of sortilin protein or Rab27a in A549 cells expressing shRNA to either pLKO control, sortilin shRNA no. 1 and no. 2 (Sh Sortilin #1, #2) and Rab27a shRNA (Sh Rab27a #1, #2). Actin expression is shown as a loading control. (C) A549 cells (2.5×10^5) were treated as detailed above. Exosomes were quantified using an ELISA-based assay of CD63 (top) or CD81 (bottom), were analyzed for statistical significance with Student *t*-test. ***$P<0.001$. (D) pLKO-A549, sortilin shRNA (ShSort1 and 2) cells were labeled with [^{35}S]methionine and [^{35}S]cysteine for 60 minutes, and chased during a time course of 0, 6 and 24 h. Exosomes were purified from the medium for each time point (apart from $t=0$ h). Exosomes (Exo) and whole-cell lysate (WCL) was solubilized in immunoprecipitation buffer and immunoprecipitated with antisera recognizing CD63. (E) Quantification of CD63 protein levels in whole-cell lysate and exosomes from pulse-chase experiment as in D ($n=3$) were analyzed for statistical significance with Student *t*-test. *$P<0.05$; **$P<0.01$; ***$P<0.001$. (F) Representative electron micrographs illustrating the morphology of MVBs and ILVs for control (pLKO) cells or cells depleted of sortilin (Sh Sortilin) or Rab27a (Sh Rab27a). Scale bars: 50 nm. Quantitative analysis of electron micrograph images showing the number of ILVs per MVB ($n=15$) and the total surface area (nm^2) of ILVs, analyzed for statistical significance with a Student's *t*-test. ***$P<0.001$. *n.s*, not significant.

(Fig. 4D, A549 Exo lane) and transferred to HUVECs (Fig. 4D, HUVEC WCL lane). We performed a control experiment to rule out the possibility that the higher molecular mass product was formed artificially during immunoprecipitation. We confirmed that this product was unable to form in a mixed immunoprecipitate of both WCL and exosomes (Fig. 4E). Given that the size of these products was much larger than the predicted size of sortilin (95 kDa) secreted from cells, these results suggested that sortilin was part of a high-molecular-mass complex. Sortilin is a multi-functional receptor that interacts with a number of ligands including the apoptotic death receptor p75 neurotrophin (p75^{NTR}, also known as NGFR) and the cell survival receptor, tropomyosin-related kinase (Trk) receptor. We screened a number of possible interacting partners by subjecting metabolic-labeled A549 cells overexpressing sortilin to co-immunoprecipitation using antibodies against sortilin, EGFR, TrkB and p75^{NTR}. We found that sortilin physically interacts with both EGFR and TrkB but not with p75^{NTR} in A549 exosomes (Fig. 4F). These results were confirmed when we performed two successive immunoprecipitations. After the first precipitation with anti-TrkB antibody under native conditions, the precipitates were released and exposed to re-immunoprecipitation with anti-EGFR antiserum followed by western blotting with anti-sortilin antibody, indicating the presence of the complex (Fig. 4G). When the first precipitation was carried out with anti-TrkB antiserum followed by precipitation with p75^{NTR} or a non-related serum, no products were detected (Fig. 4G). Taken together, these data point to a trimeric complex comprising sortilin, TrkB and EGFR, which has a predicted molecular mass of ~360–410 kDa depending on the presence of truncated (95 kDa) or full-length TrkB (145 kDa), respectively. Given that cross-talk between EGFR and TrkB has been reported previously (Qiu et al., 2006), their detection in exosomes reinforces their potential role in the cellular communication of cancer cells with the microenvironment. Hence, these results, demonstrating the presence of a new trimeric sortilin–TrkB–EGFR complex in exosomes that can be transferred to target cells, represent an important finding.

The sortilin complex in exosomes mediates communication and signaling events between A549 and endothelial cells

To elucidate whether sortilin-containing exosomes could be transferred to endothelial cells and were functionally active in the recipient cells, we investigated the effect of exosomes derived from A549 cells expressing sortilin on HUVECs. There is growing evidence that exosomes mediate cell-to-cell communication in a variety of biological processes. Hence, in addition to direct cell-to-cell interaction or secretion of active molecules, they are now considered another class of signal mediators. Exosomes contain over 400 proteins, some of which are involved in metabolism or linked to the cytoskeleton, but, most importantly, they also contain proteins involved in cell signaling pathways. The influence of these mediators on target cell signaling pathways largely remains to be elucidated (Mathivanan and Simpson, 2009). The EGFR signaling cascade modulates many pathways involved in cell proliferation, survival, adhesion, migration and differentiation (Citri and Yarden, 2006). The EGFR signaling pathway is connected to three major mitogen-activated protein kinase (MAPK)-pathways and the phosphoinositide 3-kinase (PI3K)/AKT survival pathway. The MAPK pathway consists of the ERK1/2 module, the p38 MAPK module, and the JNK module. To gain insight into the activities of these MAPK modules in HUVECs exposed to sortilin exosomes derived from A549 cells, we used arrays to analyze for the presence of phosphorylated MAPKs to explore the effect of A549 exosomes containing sortilin on signaling pathways in the target cell (Fig. 5A,B). We observed that exposure of HUVECs to A549 sortilin-containing exosomes resulted in a 3–50-fold induction (i.e. phosphorylation elevation) of several proteins involved in cell growth and differentiation such as ERK1/2 (also known as MAPK3 and MAPK1, respectively), p38δ (also known as MAPK13), AKT1/2, Hsp27, RSK1/2, GSK3α/β and JNK2 (Fig. 5A,B). Conversely, we observed a reduction in phosphorylation of all MAPK proteins analyzed when HUVECs were exposed to A549 sortilin-depleted exosomes (Fig. 5A,B). To explore further the effect of exosomes from the phenotypic cells used in this study, we chose to study a time course of several phosphorylated MAPK proteins analyzed in the array of HUVECs. We observed the phosphorylation of several kinases including ERK1/2, AKT, GAB1 and EGFR in HUVECs exposed to pLKO exosomes for 90 min (supplementary material Fig. S4A,B). We showed above that HUVECs pre-treated with dynasore or incubated at 4℃ were unable to internalize exosomes (Fig. 4A,B). However, although it was possible that the signaling pathways could be initiated from the cell surface by the binding of exosomes to the surface of the target cell, we showed that cell surface binding of exosomes to the target cell was not sufficient to transmit a signal to the target cell, as judged by reduced phosphorylation of ERK1/2, AKT, GAB1 and EGFR (supplementary material Fig. S4A,B). Likewise, phosphorylation of the MAPKs was reduced in HUVECs that were incubated with both sortilin shRNA exosomes and Rab27a shRNA exosomes (supplementary material Fig. S4A,B).

Sortilin exosomes play a role in angiogenesis

Exosomes have been associated with tumor-promoting activities. Tumor exosomes display angiogenic properties, and hypoxic tumor cells enhance angiogenesis by exosome secretion (Park et al., 2010). Exosomes have also been implicated in the activation of relevant oncogenic pathways by secretion of EGFR signaling ligands, such as amphiregulin, which is

Journal of Cell Science (2014) 127, 3983–3997 doi:10.1242/jcs.149336

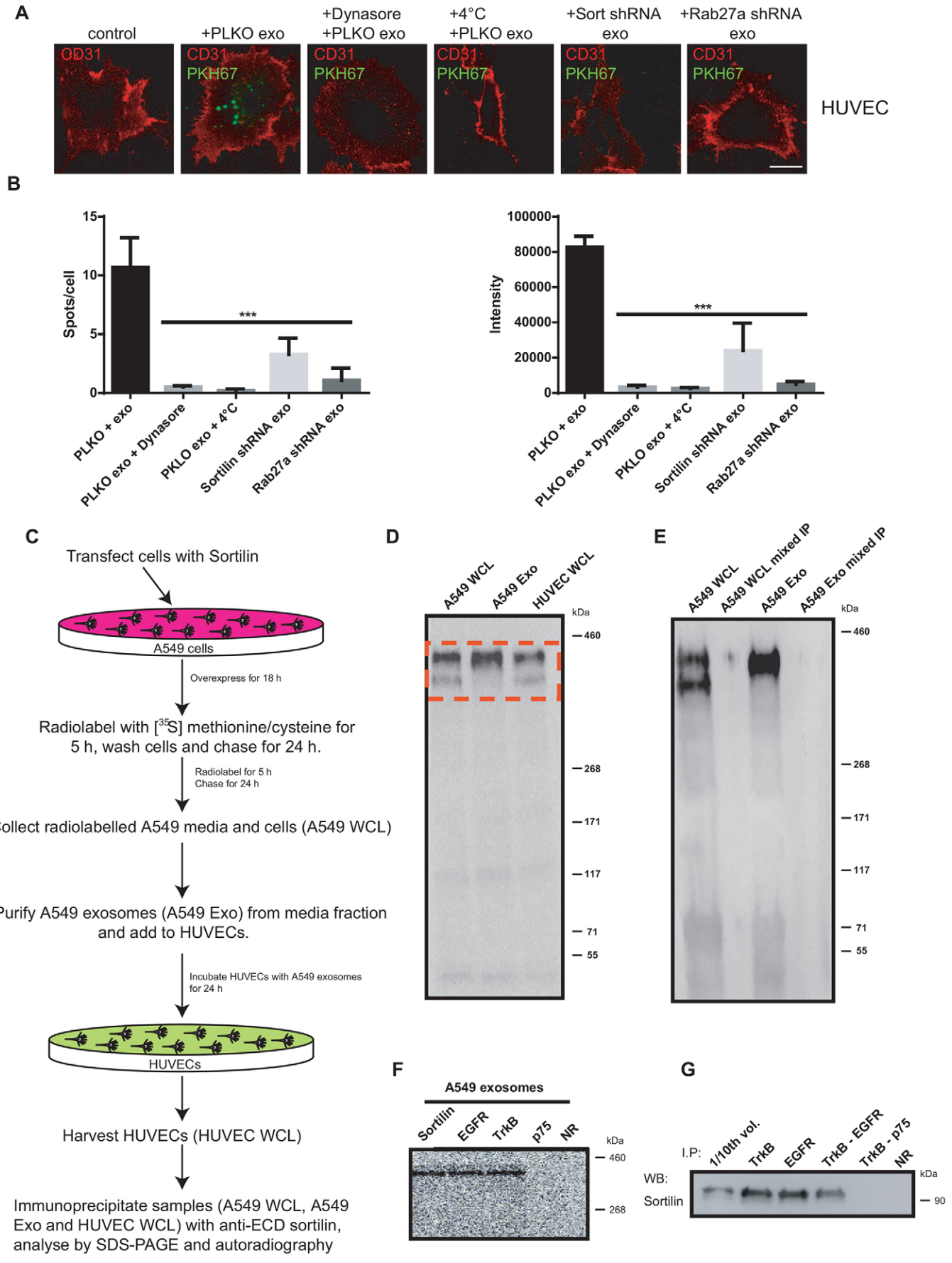

Fig. 4. See next page for legend.

Journal of Cell Science (2014) 127, 3983–3997 doi:10.1242/jcs.149336

Fig. 4. Exosomal transfer of sortilin to a target cell. (A) Exosomes purified from A549 cell lines transfected with pLKO, sortilin shRNA or Rab27a shRNA were labeled with the lipophilic dye PKH67 (in green) and added to HUVECs pre-treated with or without 40 μM dynasore. HUVECs were incubated with labeled exosomes at 37˚C or at 4˚C, and cells were fixed and analyzed by confocal microscopy. HUVECs were stained with CD31 (HUVEC marker in red). Scale bar: 20 μm. (B) Quantification of exosome uptake in HUVECs, as shown in A, measured as a spot count of labeled exosomes and fluorescence intensity of labeled exosomes ($n=3$) were analyzed for statistical significance with a Student's *t*-test. ***$P<0.001$. (C) Scheme depicting the protocol used in D. (D) A549 cells transfected with full-length (FL) sortilin for 18 h were then labeled with [^{35}S]methionine and [^{35}S]cysteine for 5 h. Cells were washed and followed by a chase for 24 h. Both radiolabeled A549 medium and whole-cell lysate (A549 WCL) were collected. Purified radiolabeled exosomes from A549 culture medium (A549 Exo) were quantified and then added at a concentration of 25 μg/ml to HUVECs. HUVECs were then incubated for 24 h and whole-cell lysate was harvested (HUVEC WCL). All samples were solubilized in immunoprecipitation buffer and immunoprecipitated with antisera recognizing the ectodomain of sortilin (anti-ECD sortilin). (E) A549 cells transfected with full-length (FL) sortilin and radiolabeled with [^{35}S]methionine and [^{35}S]cysteine as in D. In the case of mixed immunoprecipitations (A549 WCL mixed IP or A549 Exo mixed IP), two different A549 cell lines (sortilin shRNA or EGFR shRNA) were transfected with either TrkB, sortilin or EGFR. All solubilized samples of whole-cell lysate or exosomes were combined in the immunoprecipitation with antisera recognizing anti-ECD sortilin. (F) A549 cells were labeled with [^{35}S]methionine and [^{35}S]cysteine for 5 h, and chased for 24 h. Exosomes purifed from the medium were solubilized in immunoprecipitation buffer and co-immunoprecipitated (I.P.) with antisera recognizing sortilin, EGFR, TrkB, p75^{NTR} or a non-related serum (NR). (G) A western blot with anti-sortilin antibody after two successive immunoprecipitations is shown. A fraction (1/10th vol.) of the total cell lysate (used for immunoprecipitation) was included as a control.

displayed on the surface of exosomes in a signaling-competent orientation (Higginbotham et al., 2011). The presence on the surface of exosomes of active ligands for receptors, such as EGFR, which is overexpressed in many cancers, also suggests the possible involvement of exosomes in providing a favorable environment to circulating tumor cells to allow the development of metastasis (Demory Beckler et al., 2013). Cell migration is essential for many physiological processes including angiogenesis. As a functional readout of exosome activity, we assessed the effect of exosomes produced from A549 cells on recipient cancer cell invasion, a hallmark of malignancy. Using a Boyden chamber assay, we observed that pLKO-A549 (control) exosomes efficiently attracted HUVECs though the transwell, as judged by a high level of fluorescence (Fig. 6A,B). Next, we investigated the effect of sortilin-depleted A549 exosomes upon HUVEC invasion in the transwell assay. Sortilin depletion resulted in nearly a 5-fold reduction of HUVECs migrating through the chamber compared to pLKO control. Similar results were obtained for both sortilin shRNAs (shRNA no. 1, $P=0.001$; shRNA no. 2, $P=0.003$) (Fig. 6A,B). In the same way, we found that Rab27a-knockdown exosomes blocked HUVEC invasion in the transwell at a similar level (shRNA no. 1, $P=0.0009$; shRNA no. 2, $P=0.005$) to that observed for sortilin knockdown (Fig. 6A,B). We found we could significantly recover the block of HUVEC invasion imposed by sortilin-knockdown exosomes after adding back purified sortilin-containing A549 exosomes at 8 h ($P=0.01$) (Fig. 6A,B). Exosomal induction of proteins promoting angiogenesis in target cells was corroborated by the exposure of HUVECs to sortilin-containing A549 exosomes. Several relevant proteins [endothelin-1, IL-8, thrombospondin-2, urokinase-type plasminogen activator (uPA) and VEGF] were upregulated in HUVECs upon exposure to sortilin-containing

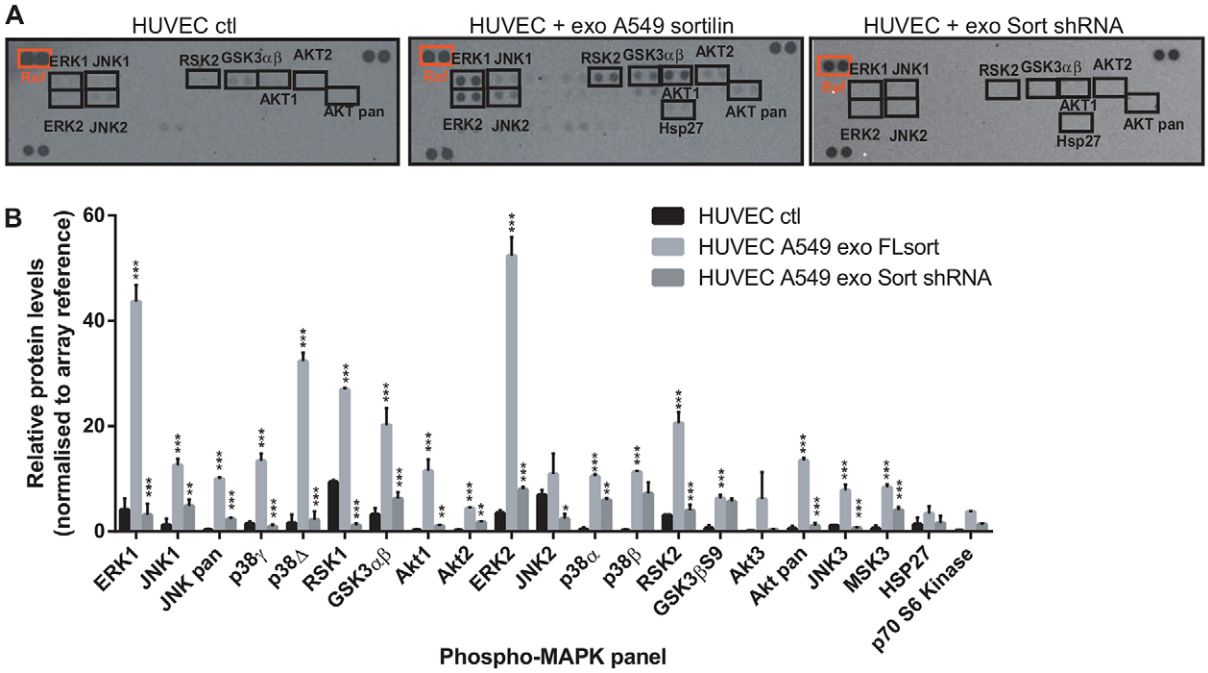

Fig. 5. Exosome transfer and signaling in the target cell. (A) A human phospho-MAPK array was used to measure the effect of exposing HUVECs to purified A549 sortilin-containing exosomes (HUVEC + exo A549 sortilin) or sortilin-depleted exosomes (HUVEC + exo A549 Sort shRNA) (25 μg/ml) upon phosphorylation of MAPKs. Representative array data are shown for HUVEC control, and HUVECs exposed to A549 sortilin-containing or sortilin-depleted exosomes. (B) Quantification of relative protein levels (normalized to array reference) in the HUVEC control and HUVECs exposed to exosomes from sortilin-containing and sortilin-depleted A549 cells ($n=3$), analyzed for statistical significance with a Student's *t*-test. *$P<0.05$; **$P<0.01$; ***$P<0.001$.

Journal of Cell Science (2014) 127, 3983–3997 doi:10.1242/jcs.149336

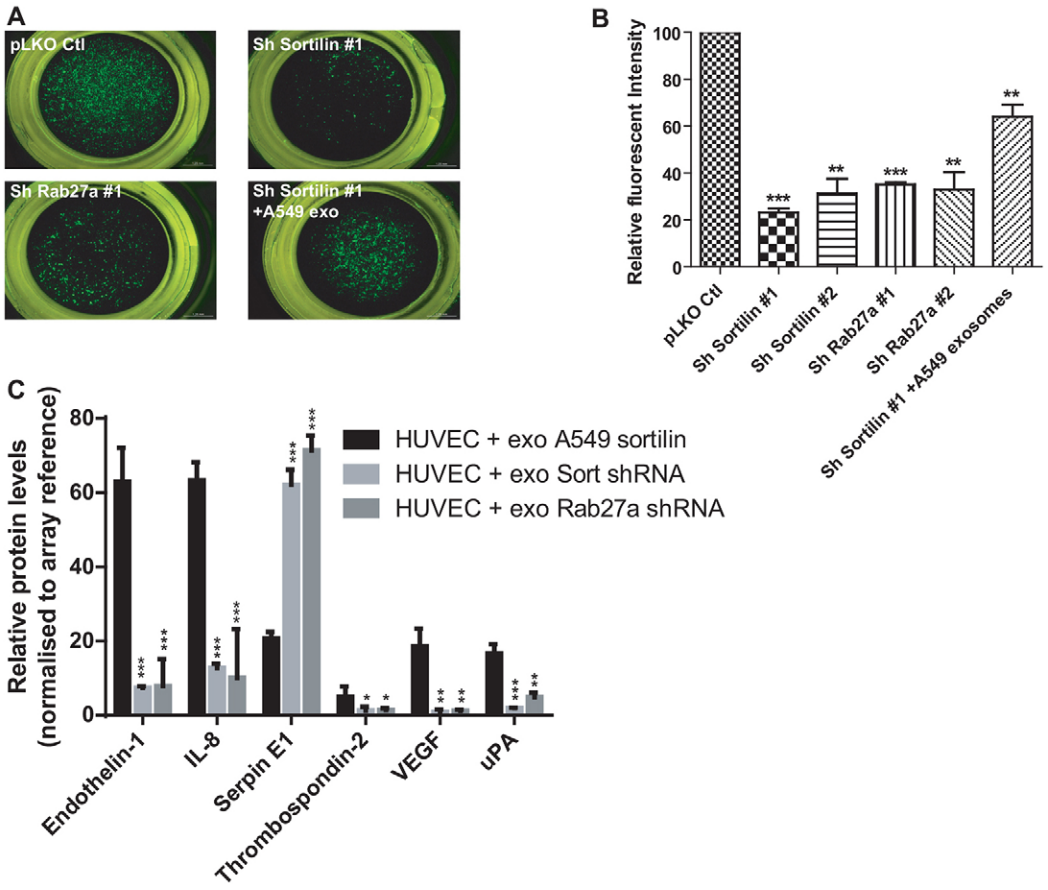

Fig. 6. Sortilin plays an autocrine function in angiogenesis. (A,B) Migration of HUVECs towards cells expressing pLKO control (Ctl), Sortilin shRNA with (+A549 exo) or without addition of sortilin-containing exosomes (25 μg/ml) and Rab27a shRNA A549 cells in a transwell Boyden chamber. (A) Representative images of the chamber. (B) Data analysis obtained from three independent Boyden experiments showing the relative fluorescent intensity and *P*-value of the different shRNAs that significantly differ from the pLKO control, were analyzed for statistical significance with a Student's *t*-test. $^{**}P<0.01$; $^{***}P<0.001$. (C) A human angiogenesis array of HUVECs exposed to exosomes from A549 sortilin (HUVEC + exo A549 sortilin), sortilin and Rab27a knockdowns A549 cells (named HUVEC + exo Sort shRNA and HUVEC + exo Rab27a shRNA). Quantification of relative protein levels (normalized to array reference) in the HUVECs exposed to exosomes from A549-sortilin, sortilin shRNA and Rab27a shRNA A549 cells ($n=3$) were analyzed for statistical significance with a Student's *t*-test. $^{*}P<0.05$; $^{**}P<0.01$; $^{***}P<0.001$.

A549 exosomes (Fig. 6C). In contrast, these same proteins were not elevated in HUVECs upon exposure to sortilin-depleted A549 exosomes (Fig. 6C). Furthermore, we observed upregulation of serpin E1 [also known as plasminogen activator inhibitor (PAI)-1] in HUVECs treated with sortilin-depleted A549 exosomes (Fig. 6C). Similar results were obtained when Rab27a-depleted A549 exosomes were used (Fig. 6C).

DISCUSSION

A role for the multifaceted receptor sortilin in exosome release and transfer is supported here by three major findings that advance our understanding of exosome release and communication with the vascular microenvironment. First, we have shown that sortilin uses exosomes for secretion and that sortilin is a key component required for exosome secretion and function (Fig. 7). Second, we identified a new heteromeric receptor complex composed of TrkB, EGFR and sortilin (herein named the TES complex) in exosomes, which mediates communication and signaling events between A549 and endothelial cells. Third, our data suggest a paracrine function for sortilin and its partners in exosome transfer and the control of the microenvironment.

The neurotensin-3 receptor sortilin plays a multitude of roles, as a receptor or co-receptor (Nykjaer et al., 2004), in protein trafficking (from the TGN to the plasma membrane and endosomes) (Chen et al., 2005) and in protein trafficking to the lysosome for protein degradation (Canuel et al., 2008). Our observation that the knockdown of sortilin affects both the number and size of ILVs found in MVBs, and their secretion into the culture medium, indicates that sortilin has a role in this process, which was previously unknown. Furthermore, we showed that the size of ILVs in the MVBs observed with sortilin shRNA is significantly larger than those observed with Rab27a shRNA. This might indicate that sortilin controls the size of exosomes and could be involved in a scission event when ILVs are formed in the MVB. There are three major steps in the formation of ILVs in the MVB where sortilin could participate in their biogenesis. The first is cargo recognition and sorting, the second is membrane budding and the third is vesicle scission from the endosome membrane. The MVB pathway is well characterized in yeast and has been shown to require the vacuolar protein sorting (*vps*) class E genes that assemble into five endosomal sorting complex required for transport (ESCRT)

Journal of Cell Science (2014) 127, 3983–3997 doi:10.1242/jcs.149336

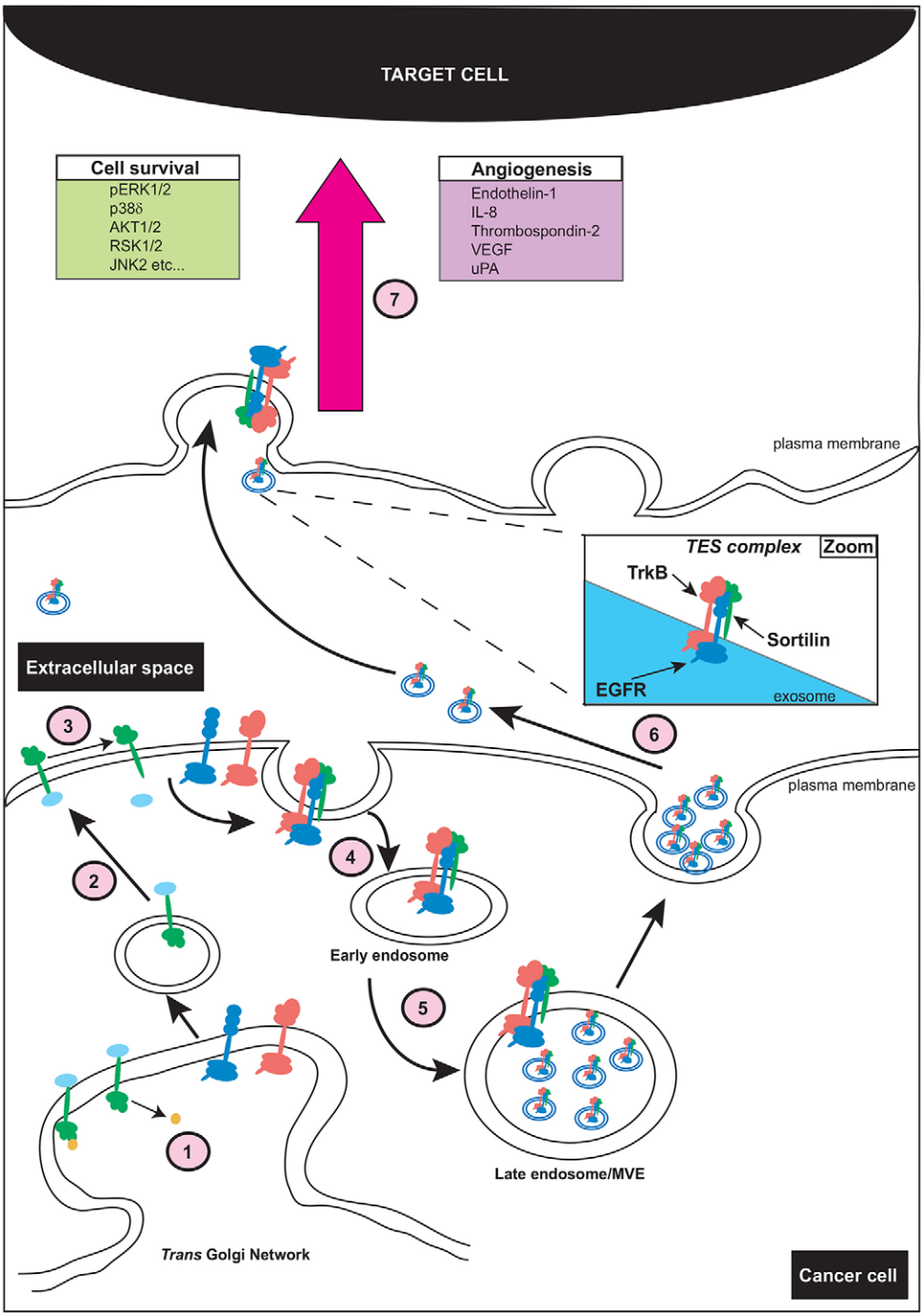

Fig. 7. The role of sortilin in exosomes. Sortilin is synthesized in the constitutive secretory pathway as a precursor encoding a short propeptide sequence. The propeptide (yellow circle) is removed by pro-protein convertases at the TGN, which facilitates the release of sortilin into the secretory pathway (step 1). There are three possible trafficking routes that sortilin could follow. Only the first is shown, whereby sortilin is transported to the cell surface via constitutive secretory vesicles (step 2). The sortilin ectodomain is cleaved by either disintegrin and metalloproteinase domain-converting protein (ADAM) 10 or ADAM17, and followed by cleavage by γ-secretase (blue oval indicating the intracellular domain, ICD) (step 3). Following shedding, sortilin forms a heterotrimeric complex with TrkB and EGFR (the TES complex) and is internalized by a clathrin-dependent endocytosis process into early endosomes (step 4). Late endosomes or multivesicular endosomes (MVEs or MVBs) containing ILVs are formed after the invagination of the multivesicular endosome membrane. These ILVs are loaded with cargo (such as the TES complex) derived from the plasma membrane and/or the cytoplasm (for example, Hsp90) (step 5). ILVs are secreted as exosomes into the extracellular space by the fusion of MVE with the plasma membrane (step 6). The exosomes primed with TES complexes are released into the extracellular space and can be taken up by target cells. The uptake of exosomes containing the TES complex mediates signaling events through the induction of the EGFR cascade and the angiogenesis process (step 7). Thus, the TES complex mediates the communication and signaling events between a cancer cell and its target cell, favoring cell proliferation, survival, adhesion, migration and differentiation through some of the proteins indicated.

complexes (ESCRT-0, ESCRT-I, ESCRT-II, ESCRT-III and Vps4) (Henne et al., 2011). The ESCRT pathway is necessary for the final membrane scission step generating the MVBs. It has been previously reported that the *HRS* gene of the ESCRT-0 complex might be involved in exosome formation and secretion (Tamai et al., 2010). A recent study has shown that silencing of genes encoding components of the ESCRT-0 complex (HRS, STAM1 or TSG101) reduces exosome secretion and alters the size and/or protein composition of the ILVs (Colombo et al., 2013). However, it still remains to be determined whether this class of proteins is important for exosome function and microenvironment control. By contrast, Rab27a plays a different role in exosome secretion; it is well documented that it is important for the docking of the MVB at the plasma membrane (Ostrowski et al., 2010). We observed that exosomes derived from sortilin- or Rab27a-depleted cells are not readily internalized by HUVECs (Fig. 4A,B). These results could be explained by the differences observed in the exosome content from exosomes derived after transfection with sortilin shRNA and Rab27a shRNA (supplementary material Fig. S2C). The sucrose density gradient analysis revealed that there were reduced protein levels of the exosome marker CD63 when sortilin or Rab27a was depleted. At the same time, the marker flotillin was maintained in sortilin-depleted exosomes, whereas it was lost upon Rab27a knockdown. Interestingly, CD63 is part of a large tetraspanin superfamily that, at the plasma membrane, can interact with cell

Journal of Cell Science (2014) 127, 3983–3997 doi:10.1242/jcs.149336

adhesion molecules such as integrins, which are involved in cell adhesion, motility and survival (Berditchevski, 2001; Pols and Klumperman, 2009). The ability of CD63 exosomes to interact with cell adhesion molecules at the plasma membrane of a target cell is not well characterized. However, it is clear that sortilin is important for exosome secretion and that the knockdown of sortilin modifies the exosome population (CD63), which might affect exosome internalization.

The role of sortilin in human neural cells was initially described as an intracellular transport protein for neurotrophins and proneurotrophins (Chen et al., 2005) and, subsequently, sortilin was shown to associate with Trk receptors (including TrkB) to enhance anterograde transport, neuronal survival and neurotrophin signaling (Vaegter et al., 2011). TrkB can bind BDNF and neurotensin-4 and -5, and is believed to be a potential target in several cancers. Although the actual mechanism of action of TrkB remains elusive, a number of studies have shown that TrkB activates PI3K/AKT and MAPK (MEK to ERK) signaling (Ho et al., 2002; Kim et al., 2004). Similarly, we observed an induction of PI3K/AKT signaling pathways in HUVECs exposed to exosomes containing sortilin and its partners EGFR and TrkB. In contrast, these same signaling pathways could be blocked when we used sortilin-depleted exosomes. These results suggest that exosomes containing the TES complex might allow communication with the microenvironment to promote cell survival and the angiogenesis process.

We observed, using a cell invasion assay, that HUVECs invading a transwell are significantly blocked in the presence of sortilin-depleted exosomes and this block is restored when supplemented with sortilin-containing exosomes. These results are not surprising, as sortilin has previously been shown to play a role in the migration (Martin et al., 2003) and release of chemokines in microglia (Dicou et al., 2004), and in dendritic spine maturation in the cerebral cortex (Gandou et al., 2010). At the same time, we demonstrate that angiogenic factors such as endothelin-1, IL-8, thrombospondin-2 and VEGF are significantly affected when we deplete sortilin from exosomes. Aberrant expression of endothelin-1, or overexpression of endothelin receptors is now recognized as a common mechanism (both autocrine and paracrine) that contributes to tumor initiation and the progression of various solid tumors, including ovarian, prostate, colon, breast, bladder and lung cancers (Rosanò et al., 2013). Interestingly, we observed a switch in the angiogenic factors with a significant elevation of serpin E1 and downregulation of uPA when HUVECs were exposed to sortilin- or Rab27a-depleted exosomes. PAI-1 has multiple roles, including cell de-adhesion, proliferation and apoptosis and cell signaling, indicating that PAI-1 expression in the tumor enhances cancer progression. Elevated levels of both uPA and PAI-1 are associated with a poor prognosis in many cancers. However, many studies have suggested that PAI-1 at a high level prevents tumor growth through inhibiting angiogenesis (McMahon et al., 2001). Taken together, our data demonstrate that the downregulation of sortilin expression in exosomes from A549 cells impairs the angiogenesis process and results in elevated levels of PAI-1 and a reduction in uPA, inhibiting the angiogenesis process.

There are unprecedented reports suggesting that disruption of the Vps10 domain proteins, including sortilin, contribute to human diseases from neurodegeneration to cancer (Wilson et al., 2014). Furthermore, the expression levels of neurotrophic factors, including their receptors, are clearly elevated in cancer, and this elevation is potentially an important factor in the angiogenesis and metastasis process. We show for the first time, a new role for sortilin in the release and the assembly of a tyrosine kinase receptor complex (TES) in lung cancer cells. Taken together, these studies and our data suggest a paracrine function for sortilin and its partners in exosome transfer and the control of the microenvironment. This new complex containing sortilin could act as a molecular switch in cancer progression by promoting angiogenesis.

MATERIALS AND METHODS

Reagents and antibodies

Cell culture reagents were from Invitrogen or Lonza. The Platinum® Quantitative PCR SuperMix-UDG was from Invitrogen, and the EasyTag Express Protein Labeling L-[^{35}S] methionine/cysteine mix were from PerkinElmer. All other chemicals were from Sigma, Ozyme and BD Bioscience. Rabbit polyclonal antisera recognizing sortilin was kindly provided by Claus Munck Petersen (Aahrus University, Denmark). Antisera used in FACS analysis were: mouse anti-human-CD63 (BD Bioscience) antibodies, for coupling to beads, and FITC-conjugated anti-CD63 and anti-CD81 (Biolegend) and rat anti-EGFR antibodies (Serotec). Antisera used for immunoblotting were: mouse anti-ECD-Sortilin (BD Bioscience); rabbit anti-p75^{NTR} and goat anti-ICD-sortilin (Santa Cruz Biotechnology); mouse anti-CD63 (Serotec); rabbit anti-Rab27a (Sigma); rabbit anti-EEA1 (Sigma); rabbit anti-flotillin and anti-TrkB (Cell Signaling); mouse anti-actin (Sigma); mouse anti-V5 and anti-GFP (Life Technologies); and horseradish peroxidase (HRP)-conjugated secondary antibodies (Dako).

cDNA constructs

Full-length human sortilin cDNA, V5- and GFP-tagged fusion proteins cloned in pEF6/V5-His TOPO vector or the pcDNA3.1/CTGFP TOPO vector were generously provided by Tae-Wan Kim (Columbia University Medical Center, NY). Lentiviral vector pCT-CD63-GFP expressing a CD63–GFP fusion protein was obtained from BioCat.

Cell culture and treatments

HUVECs (purchased from Lonza) were cultured in endothelial cell growth medium containing 2% fetal bovine serum (FBS) (EGM-2; Lonza) and growth factors. Human lung carcinoma cell line (A549) and human embryonic kidney 293 cells (HEK293T) were purchased from ATCC and maintained in DMEM GlutaMAX™ (Invitrogen) supplemented with 10% FBS and 1% non-essential amino acids. All cells were cultured in a humidified incubator set at 5% CO_2 and 37℃. For chemical compound treatments, in brief, A549 cells (2.5×10^5) were transfected or not in six-well plates and treated with 2.5 µg/ml tunicamycin, 1 µg/ml brefeldin A (BFA), 15 nM dimethyl amiloride (DMA) or 2 µM Monensin (Mon) for 24 h.

Overexpression and lentivirus-mediated RNA interference

For both transient and stable transfection, cells were transfected using JetPei transfection reagent (Polyplus transfection, Ozyme). Lentivirus-mediated RNA interference was used to generate sortilin-knockdown and Rab27a-knockdown stable cell lines using the previously described procedure (Magnaudeix et al., 2013). The shRNA sequences were as follows: for sortilin, TRCN0000005295 (5′-CCGGCCAGTGTACTT-TACCAATATACTCGAGTATATTGGTAAAGTACACTGGTTTTT-3′) and TRCN0000005296 (5′-CCGGCGGATCAGTTAAGTGAAGAAA-CTCGAGTTTCTTCACTTAACTGATCCGTTTTT-3′); and for Rab27a, TRCN0000005295 (5′-CCGGCCAGTGTACTTTACCAATATACTCG-AGTATATTGGTAAAGTACACTGGTTTTT-3′) and TRCN0000005296 (5′-CCGGCGGATCAGTTAAGTGAAGAAACTCGAGTTTCTTCACT-TAACTGATCCGTTTTT-3′).

Quantitative reverse transcription-PCR

The Qiagen RNeasy kit was used to isolate total RNA from cells at day 15 after lentiviral infection. Single-stranded cDNA was prepared using the high capacity cDNA reverse transcription kit according to the manufacturer's protocol (Applied Biosystems). The reaction was stopped

by incubation at 95℃ for 5 min. Approximately of 100 ng cDNA was used for each PCR reaction, performed with TaqMan (Applied Biosystems) on an ABI Step One Plus real-time thermal cycler (Applied Biosystems). PCR primers for sortilin, Rab27a and GAPDH were designed and used for the PCR amplification with Taq DNA polymerase (Roche Diagnostics).

Metabolic labeling and A549–HUVEC exosome transfer

For A549–HUVEC exosome transfer, A549 cells grown in 10-cm^2 Petri dishes were transfected with full-length sortilin for 18 h prior to metabolic labeling; for the pulse-chase time course experiments, cells were grown in six-well dishes. Cells were starved for 20 min in methionine- and cysteine-free DMEM (Invitrogen) with 2 mM glutamine, and then metabolically labeled with the same medium containing 20 µCi/ml of [^{35}S]methionine and [^{35}S]cysteine (1175 Ci/mmol, 11.9 mCi/ml) protein labeling mix for 60 min (time course) or for 300 min (exosome transfer). Cells were rinsed twice with PBS, and fresh DMEM Glutamax medium was added or solubilized in Triton X-100 immunoprecipitation buffer (Wilson et al., 2000; Wilson et al., 2008) containing 1 mM PMSF and 1 mM non-radioactive methionine and cysteine for timecourse experiments at t=0 h. For pulse-chase time course experiments, cells were incubated for 6 and 24 h, and both cell lysates and medium were harvested. For exosome transfer, cells were then incubated in fresh complete DMEM Glutamax medium for 24 h and metabolically labeled exosomes were harvested from the medium samples as detailed below. Labeled exosomes (25 µg/ml) were added to the medium of cultured endothelial cells HUVECs for a further 24 h before harvesting both the cell lysates and medium. Samples were precleared and immunoprecipitated with specific antisera prior to SDS-PAGE and autoradiography or phosphoimaging.

Indirect immunofluorescence and confocal microscopy analysis

Cells grown on glass coverslips (14-mm diameter, Menzel-Gläser, VWR, Fontenay-sous-Bois, France) were fixed using methanol or 2% paraformaldehyde for 10 min, washed with PBS solution containing 1% (w/v) BSA and blocked with PBS with BSA solution for 30 min followed by staining with the indicated primary antibody at room temperature for 2 h, and, subsequently, either with anti-rabbit-IgG Alexa-Fluor-594-conjugated or anti-mouse-IgG Alexa-Fluor-488-conjugated antibodies (1:200; Invitrogen) for 45 min at room temperature. For PKH67 (Sigma) staining, exosomes were incubated for 5 min at room temperature. The staining reaction was stopped after 5 min with exosome-free FCS. Exosomes were then washed in PBS and pelleted by ultracentrifugation (100,000 ***g***, 1 h). For DiI (1,1′-dioctadecyl-3,3,3′3′-tetramethylindocarbocyanine perchlorate) (Molecular Probes, France) staining of A549 cells transfected with CD63–GFP, cells were incubated with 1 µM DiI for 2 h at 37℃. Fluorescence images were obtained using a charge-coupled device camera (Photonic Science) driven by Visiolab 2000 software (Biocom) or by using an epifluorescence microscope (Zeiss Axiovert-200) equipped with a laser-scanning confocal imaging system (Zeiss LSM 510 META).

Immunoadsorption and detection of exosomes by FACS

Anti-human-CD63 antibody was coupled to 4.5-µm aldehyde-sulfate beads (Invitrogen) by incubating 35 µg of antibody with 1×10^8 beads followed by blocking of remaining activated groups with PBS containing 4% BSA. Cell culture supernatants were cleared by centrifugation at 18,000 ***g*** (for 20 min). Cleared supernatants (100 µl) were incubated with 20,000 anti-CD63-coupled beads overnight at room temperature with 200 rpm horizontal shaking. Beads were washed twice in PBS containing 2% BSA and were incubated with FITC-conjugated anti-CD81 (Biolegend) or anti-EGFR antibody (Serotec) for 1 h at room temperature. Beads were washed twice in PBS containing 2% BSA. Beads were acquired on a FACSCalibur (BD) and data were analyzed with CellQuest software (BD). The threshold of negative staining was obtained with beads incubated with unconditioned medium, and for each culture condition, the amount of exosomes was calculated in arbitrary units (AU) as a percentage of positive beads.

MVB purification and characterization

Exosomes were isolated from the cell culture medium by differential centrifugation. Briefly, cells were cultured for the time periods as indicated in figure legends in exosome-free medium and centrifuged at 300 ***g*** for 5 min at 4℃ to remove cell debris. Supernatants were further centrifuged at 16,500 ***g*** for 30 min at 4℃. Next, exosomes were pelleted by ultracentrifugation at 100,000 ***g*** for 2 h at 4℃, washed in PBS and re-centrifuged at 100,000 ***g*** for 2 h at 4℃. For each exosome preparation, the concentration of total proteins was quantified with the Bio-Rad protein assay kit. Exosomes were then resuspended in an appropriate volume of PBS for further analysis or used for protein isolation.

Quantification of exosome particles

Exosome particles harvested from culture medium were quantified using either the CD63 or CD81 ELISA kit (System Biosciences, Ozyme, France). Exosome pellets were resuspended in 100 µl Exosome Binding buffer and analyzed according to the manufacturer's instructions.

Microarray

To investigate phosphorylated kinases or the angiogenesis pathway we used Proteome Profiler^{TM} arrays (R&D Systems, Wiesbaden, Germany). In brief, cells grown in 10-cm^2 Petri dishes were either transfected or not with full-length sortilin for 18 h and the medium was refreshed with fresh complete DMEM Glutamax medium for a further 24 h. Exosomes were purified by differential ultracentrifugation and were added (25 µg/ml) or not to the medium of cultured endothelial cells HUVECs for a further 24 h before harvesting the cell lysates. Samples were lysed in RIPA buffer supplemented with protease inhibitor cocktail. Total protein from HUVEC lysates (300 µg) was analyzed using the human phospho-MAPK or the human angiogenesis antibody array (R&D Systems). The arrays were scanned and quantified with ImageJ software (NIH, Bethesda, MD). All of the arrays were performed according to the manufacturer's recommendations.

Invasion assays

Invasion assays were performed in a BD Biocoat Matrigel invasion chamber with an 8-µm diameter pore size membrane and a thin layer of Matrigel, in a 24-well plate. Inserts were rehydrated for 2 h in EGM-2 medium. After detachment of confluent cells with trypsin and EDTA, HUVECs (5×10^4) were seeded in the upper surface of the transwell plates with A549, and sortilin- or Rab27a-knockdown A549 cells were added to the lower chamber and cultured for 24 h at 37℃ under 5% CO_2. After incubation, the lower chamber was treated with 50 µM calcein AM fluorescent dye for 30 min at 37℃ and under 5% CO_2. Non-invading cells in the upper part of the insert were carefully removed. Three independent assays were performed, and cells were seeded in triplicate for each cell line. Invading cells were measured using a Twinkle LB 970 Microplate Fluorometer (Berthold Technologies) and images were obtained using a fluorescence microscope M2FLIII (Leica). Results are presented as mean±s.d. for each sample, and invasion levels obtained were compared with the pKLO control cell line.

Statistical analysis

Treatments, relative fluorescence intensities, antibody arrays and western blotting experiments were compared with control using Statview software (Statview v.5.0). Data shown are representative of at least three independent experiments. Error bars represent by s.e.m. Results were analyzed for statistical significance by one-way ANOVA or Student's t-test. $P<0.05$ was considered as significant, with actual values represented by asterisks (*$P<0.05$; **$P<0.01$; ***$P<0.001$).

Acknowledgements

We are grateful to all our colleagues who have contributed their time and materials towards this paper. We especially thank the technical support of the electron microscopy service of CHU Poitiers and Imaging Cytometry Platform of the University of Limoges.

Competing interests

The authors declare no competing interests.

Author contributions

C.M.W. and T.N. executed the experiments and analyzed the data. C.M.W., T.N., F.V., B.M., F.B. and M.-O.J. participated in the design. C.M.W., T.N., F.V., F.L., and M.-O.J coordinated the study. All authors read and approved the final manuscript.

Funding

This study was generously supported by Chaire de Pneumologie Expérimentale from Association Limousine d'Aide aux Insuffisants Respiratoires-Assistance Ventilatoire à domicile (ALAIR-AVD; Limousin, France); and the Fondation of the University of Limoges.

Supplementary material

Supplementary material available online at
http://jcs.biologists.org/lookup/suppl/doi:10.1242/jcs.149336/-/DC1

References

Babst, M., Odorizzi, G., Estepa, E. J. and Emr, S. D. (2000). Mammalian tumor susceptibility gene 101 (TSG101) and the yeast homologue, Vps23p, both function in late endosomal trafficking. *Traffic* **1**, 248-258.

Berditchevski, F. (2001). Complexes of tetraspanins with integrins: more than meets the eye. *J. Cell Sci.* **114**, 4143-4151.

Bobrie, A., Colombo, M., Krumeich, S., Raposo, G. and Thery, C. (2012). Diverse subpopulations of vesicles secreted by different intracellular mechanisms are present in exosome preparations obtained by differential ultracentrifugation. *J. Extracell. Vesicles* **1**, 18397.

Canuel, M., Korkidakis, A., Konnyu, K. and Morales, C. R. (2008). Sortilin mediates the lysosomal targeting of cathepsins D and H. *Biochem. Biophys. Res. Commun.* **373**, 292-297.

Chen, Z. Y., Ieraci, A., Teng, H., Dall, H., Meng, C. X., Herrera, D. G., Nykjaer, A., Hempstead, B. L. and Lee, F. S. (2005). Sortilin controls intracellular sorting of brain-derived neurotrophic factor to the regulated secretory pathway. *J. Neurosci.* **25**, 6156-6166.

Citri, A. and Yarden, Y. (2006). EGF-ERBB signalling: towards the systems level. *Nat. Rev. Mol. Cell Biol.* **7**, 505-516.

Colombo, M., Moita, C., van Niel, G., Kowal, J., Vigneron, J., Benaroch, P., Manel, N., Moita, L. F., Théry, C. and Raposo, G. (2013). Analysis of ESCRT functions in exosome biogenesis, composition and secretion highlights the heterogeneity of extracellular vesicles. *J. Cell Sci.* **126**, 5553-5565.

Dal Farra, C., Sarret, P., Navarro, V., Botto, J. M., Mazella, J. and Vincent, J. P. (2001). Involvement of the neurotensin receptor subtype NTR3 in the growth effect of neurotensin on cancer cell lines. *Int. J. Cancer* **92**, 503-509.

Demory Beckler, M., Higginbotham, J. N., Franklin, J. L., Ham, A. J., Halvey, P. J., Imasuen, I. E., Whitwell, C., Li, M., Liebler, D. C. and Coffey, R. J. (2013). Proteomic analysis of exosomes from mutant KRAS colon cancer cells identifies intercellular transfer of mutant KRAS. *Mol. Cell. Proteomics* **12**, 343-355.

Dicou, E., Vincent, J. P. and Mazella, J. (2004). Neurotensin receptor-3/sortilin mediates neurotensin-induced cytokine/chemokine expression in a murine microglial cell line. *J. Neurosci. Res.* **78**, 92-99.

Escola, J. M., Kleijmeer, M. J., Stoorvogel, W., Griffith, J. M., Yoshie, O. and Geuze, H. J. (1998). Selective enrichment of tetraspan proteins on the internal vesicles of multivesicular endosomes and on exosomes secreted by human B-lymphocytes. *J. Biol. Chem.* **273**, 20121-20127.

Finan, G. M., Okada, H. and Kim, T. W. (2011). BACE1 retrograde trafficking is uniquely regulated by the cytoplasmic domain of sortilin. *J. Biol. Chem.* **286**, 12602-12616.

Gandou, C., Ohtani, A., Senzaki, K. and Shiga, T. (2010). Neurotensin promotes the dendrite elongation and the dendritic spine maturation of the cerebral cortex in vitro. *Neurosci. Res.* **66**, 246-255.

Giorgi, R. R., Chile, T., Bello, A. R., Reyes, R., Fortes, M. A., Machado, M. C., Cescato, V. A., Musolino, N. R., Bronstein, M. D., Giannella-Neto, D. et al. (2008). Expression of neurotensin and its receptors in pituitary adenomas. *J. Neuroendocrinol.* **20**, 1052-1057.

Henne, W. M., Buchkovich, N. J. and Emr, S. D. (2011). The ESCRT pathway. *Dev. Cell* **21**, 77-91.

Hermey, G., Sjøgaard, S. S., Petersen, C. M., Nykjaer, A. and Gliemann, J. (2006). Tumour necrosis factor alpha-converting enzyme mediates ectodomain shedding of Vps10p-domain receptor family members. *Biochem. J.* **395**, 285-293.

Higginbotham, J. N., Demory Beckler, M., Gephart, J. D., Franklin, J. L., Bogatcheva, G., Kremers, G. J., Piston, D. W., Ayers, G. D., McConnell, R. E., Tyska, M. J. et al. (2011). Amphiregulin exosomes increase cancer cell invasion. *Curr. Biol.* **21**, 779-786.

Ho, R., Eggert, A., Hishiki, T., Minturn, J. E., Ikegaki, N., Foster, P., Camoratto, A. M., Evans, A. E. and Brodeur, G. M. (2002). Resistance to chemotherapy mediated by TrkB in neuroblastomas. *Cancer Res.* **62**, 6462-6466.

Kim, H., Li, Q., Hempstead, B. L. and Madri, J. A. (2004). Paracrine and autocrine functions of brain-derived neurotrophic factor (BDNF) and nerve growth factor (NGF) in brain-derived endothelial cells. *J. Biol. Chem.* **279**, 33538-33546.

Lippincott-Schwartz, J., Yuan, L. C., Bonifacino, J. S. and Klausner, R. D. (1989). Rapid redistribution of Golgi proteins into the ER in cells treated with brefeldin A: evidence for membrane cycling from Golgi to ER. *Cell* **56**, 801-813.

Magnaudeix, A., Wilson, C. M., Page, G., Bauvy, C., Codogno, P., Lévêque, P., Labrousse, F., Corre-Delage, M., Yardin, C. and Terro, F. (2013). PP2A blockade inhibits autophagy and causes intraneuronal accumulation of ubiquitinated proteins. *Neurobiol. Aging* **34**, 770-790.

Martin, S., Vincent, J. P. and Mazella, J. (2003). Involvement of the neurotensin receptor-3 in the neurotensin-induced migration of human microglia. *J. Neurosci.* **23**, 1198-1205.

Massa, F., Devader, C., Béraud-Dufour, S., Brau, F., Coppola, T. and Mazella, J. (2013). Focal adhesion kinase dependent activation of the PI3 kinase pathway by the functional soluble form of neurotensin receptor-3 in HT29 cells. *Int. J. Biochem. Cell Biol.* **45**, 952-959.

Mathivanan, S. and Simpson, R. J. (2009). ExoCarta: A compendium of exosomal proteins and RNA. *Proteomics* **9**, 4997-5000.

McMahon, G. A., Petitclerc, E., Stefansson, S., Smith, E., Wong, M. K., Westrick, R. J., Ginsburg, D., Brooks, P. C. and Lawrence, D. A. (2001). Plasminogen activator inhibitor-1 regulates tumor growth and angiogenesis. *J. Biol. Chem.* **276**, 33964-33968.

Mendelsohn, J. and Baselga, J. (2003). Status of epidermal growth factor receptor antagonists in the biology and treatment of cancer. *J. Clin. Oncol.* **21**, 2787-2799.

Navarro, V., Vincent, J. P. and Mazella, J. (2002). Shedding of the luminal domain of the neurotensin receptor-3/sortilin in the HT29 cell line. *Biochem. Biophys. Res. Commun.* **298**, 760-764.

Nielsen, M. S., Madsen, P., Christensen, E. I., Nykjaer, A., Gliemann, J., Kasper, D., Pohlmann, R. and Petersen, C. M. (2001). The sortilin cytoplasmic tail conveys Golgi-endosome transport and binds the VHS domain of the GGA2 sorting protein. *EMBO J.* **20**, 2180-2190.

Nykjaer, A. and Willnow, T. E. (2012). Sortilin: a receptor to regulate neuronal viability and function. *Trends Neurosci.* **35**, 261-270.

Nykjaer, A., Lee, R., Teng, K. K., Jansen, P., Madsen, P., Nielsen, M. S., Jacobsen, C., Kliemannel, M., Schwarz, E., Willnow, T. E. et al. (2004). Sortilin is essential for proNGF-induced neuronal cell death. *Nature* **427**, 843-848.

Ostrowski, M., Carmo, N. B., Krumeich, S., Fanget, I., Raposo, G., Savina, A., Moita, C. F., Schauer, K., Hume, A. N., Freitas, R. P. et al. (2010). Rab27a and Rab27b control different steps of the exosome secretion pathway. *Nat. Cell Biol.* **12**, 19-30; **Suppl.** 11-13.

Pan, B. T., Teng, K., Wu, C., Adam, M. and Johnstone, R. M. (1985). Electron microscopic evidence for externalization of the transferrin receptor in vesicular form in sheep reticulocytes. *J. Cell Biol.* **101**, 942-948.

Park, J. E., Tan, H. S., Datta, A., Lai, R. C., Zhang, H., Meng, W., Lim, S. K. and Sze, S. K. (2010). Hypoxic tumor cell modulates its microenvironment to enhance angiogenic and metastatic potential by secretion of proteins and exosomes. *Mol. Cell. Proteomics* **9**, 1085-1099.

Peinado, H., Alečković, M., Lavotshkin, S., Matei, I., Costa-Silva, B., Moreno-Bueno, G., Hergueta-Redondo, M., Williams, C., García-Santos, G., Ghajar, C. et al. (2012). Melanoma exosomes educate bone marrow progenitor cells toward a pro-metastatic phenotype through MET. *Nat. Med.* **18**, 883-891.

Pols, M. S. and Klumperman, J. (2009). Trafficking and function of the tetraspanin CD63. *Exp. Cell Res.* **315**, 1584-1592.

Qiu, L., Zhou, C., Sun, Y., Di, W., Scheffler, E., Healey, S., Kouttab, N., Chu, W. and Wan, Y. (2006). Crosstalk between EGFR and TrkB enhances ovarian cancer cell migration and proliferation. *Int. J. Oncol.* **29**, 1003-1011.

Raposo, G. and Stoorvogel, W. (2013). Extracellular vesicles: exosomes, microvesicles, and friends. *J. Cell Biol.* **200**, 373-383.

Raposo, G., Nijman, H. W., Stoorvogel, W., Liejendekker, R., Harding, C. V., Melief, C. J. and Geuze, H. J. (1996). B lymphocytes secrete antigen-presenting vesicles. *J. Exp. Med.* **183**, 1161-1172.

Record, M., Carayon, K., Poirot, M. and Silvente-Poirot, S. (2014). Exosomes as new vesicular lipid transporters involved in cell-cell communication and various pathophysiologies. *Biochim. Biophys. Acta* **1841**, 108-120.

Rosanò, L., Spinella, F. and Bagnato, A. (2013). Endothelin 1 in cancer: biological implications and therapeutic opportunities. *Nat. Rev. Cancer* **13**, 637-651.

Savina, A., Furlán, M., Vidal, M. and Colombo, M. I. (2003). Exosome release is regulated by a calcium-dependent mechanism in K562 cells. *J. Biol. Chem.* **278**, 20083-20090.

Simons, M. and Raposo, G. (2009). Exosomes – vesicular carriers for intercellular communication. *Curr. Opin. Cell Biol.* **21**, 575-581.

Tamai, K., Tanaka, N., Nakano, T., Kakazu, E., Kondo, Y., Inoue, J., Shiina, M., Fukushima, K., Hoshino, T., Sano, K. et al. (2010). Exosome secretion of dendritic cells is regulated by Hrs, an ESCRT-0 protein. *Biochem. Biophys. Res. Commun.* **399**, 384-390.

Théry, C., Ostrowski, M. and Segura, E. (2009). Membrane vesicles as conveyors of immune responses. *Nat. Rev. Immunol.* **9**, 581-593.

Truzzi, F., Marconi, A., Lotti, R., Dallaglio, K., French, L. E., Hempstead, B. L. and Pincelli, C. (2008). Neurotrophins and their receptors stimulate melanoma cell proliferation and migration. *J. Invest. Dermatol.* **128**, 2031-2040.

Vaegter, C. B., Jansen, P., Fjorback, A. W., Glerup, S., Skeldal, S., Kjolby, M., Richner, M., Erdmann, B., Nyengaard, J. R., Tessarollo, L. et al. (2011). Sortilin associates with Trk receptors to enhance anterograde transport and neurotrophin signaling. *Nat. Neurosci.* **14**, 54-61.

Wilson, C. M., Farmery, M. R. and Bulleid, N. J. (2000). Pivotal role of calnexin and mannose trimming in regulating the endoplasmic reticulum-associated

degradation of major histocompatibility complex class I heavy chain. *J. Biol. Chem.* **275**, 21224-21232.

Wilson, C. M., Roebuck, Q. and High, S. (2008). Ribophorin I regulates substrate delivery to the oligosaccharyltransferase core. *Proc. Natl. Acad. Sci. USA* **105**, 9534-9539.

Wilson, C. M., Magnaudeix, A., Yardin, C. and Terro, F. (2011). DC2 and keratinocyte-associated protein 2 (KCP2), subunits of the oligosaccharyltransferase complex, are regulators of the gamma-secretase-directed processing of amyloid precursor protein (APP). *J. Biol. Chem.* **286**, 31080-31091.

Wilson, C. M., Naves, T., Saada, S., Pinet, S., Vincent, F., Lalloué, F. and Jauberteau, M. O. (2014). The implications of Sortilin/Vps10p domain receptors in neurological and human diseases. *CNS Neurol. Disord. Drug Targets*. (in press)

Zhang, S., Guo, D., Luo, W., Zhang, Q., Zhang, Y., Li, C., Lu, Y., Cui, Z. and Qiu, X. (2010). TrkB is highly expressed in NSCLC and mediates BDNF-induced the activation of Pyk2 signaling and the invasion of A549 cells. *BMC Cancer* **10**, 43.